Chapter 10

Decadal variability of the Indian Ocean and its predictability[⍟]

Tomoki Tozuka[a], Lu Dong[b], Weiqing Han[c], Matthieu Lengaigne[d], and Lei Zhang[e,f]

[a]*Department of Earth and Planetary Science, Graduate School of Science, The University of Tokyo, Tokyo, Japan,* [b]*Frontier Science Centre for Deep Ocean Multispheres and Earth System and Physical Oceanography Laboratory, Ocean University of China, Qingdao, People's Republic of China,* [c]*Department of Atmospheric and Oceanic Sciences, University of Colorado, Boulder, CO, United States,* [d]*MARBEC, University of Montpellier, CNRS, IFREMER, IRD, Sète, France,* [e]*State Key Laboratory of Tropical Oceanography, South China Sea Institute of Oceanology, Chinese Academy of Sciences, Guangzhou, Guangdong, People's Republic of China,* [f]*Global Ocean and Climate Research Center, South China Sea Institute of Oceanology, Guangzhou, Guangdong, People's Republic of China*

1 Introduction

The Indian Ocean exhibits variations across different timescales, with decadal variations (encompassing periods ranging from approximately 7 years to several decades) being the least understood. Unlike the Pacific Ocean, which has been extensively studied for its Pacific Decadal Oscillation (PDO) and/or Interdecadal Pacific Oscillation (IPO) (Newman, 2016; Power, 2021), and the Atlantic Ocean, which has received significant attention for its Atlantic multidecadal variability (Sutton et al., 2018), the modes of decadal internal climate variability in the Indian Ocean remain a "gray area" due to limited data and dedicated research (Han et al., 2014). However, this does not imply that the Indian Ocean is devoid of decadal variations. On the contrary, it poses a serious challenge when attributing climate change signals specific to the region. To overcome this challenge, there is a pressing need to thoroughly characterize the natural decadal variability of the Indian Ocean, enabling us to attribute regional climate change signals accurately and enhance our global climate prediction capabilities for the coming decades.

There has been renewed interest in Indian Ocean decadal variability recently due to its potential involvement in the recent global surface warming "hiatus" (England, 2014; Kosaka & Xie, 2013). It is believed that the negative IPO phase played a crucial role by causing increased heat absorption in the tropical Pacific, but also a rapid surface warming in the Indian Ocean, which in turn, likely contributed to this negative IPO phase by enhancing the Walker circulation (Dong & McPhaden, 2017a; Hamlington et al., 2014; Han et al., 2017a; Li & Han, 2015; Luo et al., 2012; Zhang et al., 2019). Additionally, a substantial fraction of the Pacific heat uptake has been transported to the Indian Ocean through the Indonesian Throughflow (ITF; Lee et al., 2015; Nieves et al., 2015; Zhang et al., 2018b). Consequently, the Indian Ocean has been responsible for more than 70% of the increase in global oceanic heat content within the upper 700 m during the past decade (Lee et al., 2015). The fate of this extra heat in the Indian Ocean—whether it re-surfaces or remains at depth in the upcoming decades—has the potential to influence the evolution of global surface temperature (Vialard, 2015). As a result, the Indian Ocean emerges as a region of significant importance for decadal climate predictions.

This chapter aims to present an up-to-date review of progress made in our understanding of Indian Ocean decadal variability since a seminal review paper by Han et al. (2014). Addressing outstanding questions raised in that review paper is a key focus, particularly exploring the relative importance of external forcing and internal variability within the Indian Ocean in generating decadal fluctuations. This chapter is organized as follows: the next section delves into what instrumental records reveal about decadal variability in the Indian Ocean. Sections 3 and 4 then offer comprehensive reviews of recent advancements in understanding internal and externally forced decadal climate variability, respectively. Section 5 presents the latest findings on decadal climate predictions. Conclusions and noteworthy unresolved questions are discussed in the final section. It is important to note that this chapter only provides brief mentions of decadal variability in biogeochemical variables

[⍟]This book has a companion website hosting complementary materials. Visit this URL to access it: https://www.elsevier.com/books-and-journals/book-companion/9780128226988.

The Indian Ocean and its Role in the Global Climate System. https://doi.org/10.1016/B978-0-12-822698-8.00014-7

(for more details, see Al-Yamani et al., 2024; Hood et al., 2024a), decadal variations recorded in paleoclimate proxies (Mohtadi et al., 2024), future climate projections (Roxy et al., 2024), and impact of Indian Ocean decadal/multidecadal signals on regional and global climate (Ummenhofer et al., 2024) as these aspects are reviewed more extensively in other chapters.

2 Observational datasets

Data sparsity before 1980. To investigate the decadal variability of the Indian Ocean and differentiate it from externally forced long-term climate change signals, comprehensive and consistent climate observations spanning the entire basin are essential. However, the availability of high-resolution instrumental climate datasets with global coverage has been limited to the introduction of satellites in the late 1970s. Before that, the instrumental records of climate variables were characterized by significant uncertainties due to the scarcity of observations and the presence of time-varying biases in the collected data (Parker et al., 2000). As a consequence, studying Indian Ocean decadal variability before the satellite era poses considerable challenges, primarily due to the lack of reliable and homogeneous data.

SST and tide gauges. Sea surface temperature (SST) stands as a vital variable in studying decadal climate variability, owing to its key role in large-scale atmosphere-ocean interactions. The instrumental record of SST dates back to the mid-19th century. However, the spatial coverage during earlier periods was generally inadequate, with SST measurements mostly restricted to shipping lanes (Fig. 1a). Although the coverage expanded to more areas in the 20th century, certain areas, such as the tropics and the Southern Ocean, still exhibit poor data coverage (Fig. 1b and c). Another pertinent example is the global sea level record derived from tide gauges (Fig. 1d), which offers essential information for studying both regional and global scale sea level changes (Han, 2010; Unnikrishnan & Shankar, 2007). While some tide gauge data provide more than a century of continuous sea level records—surpassing the duration of satellite-derived products—their utility is limited for analyzing basin-scale climate variations due to coarse spatial sampling. Consequently, data sparsity

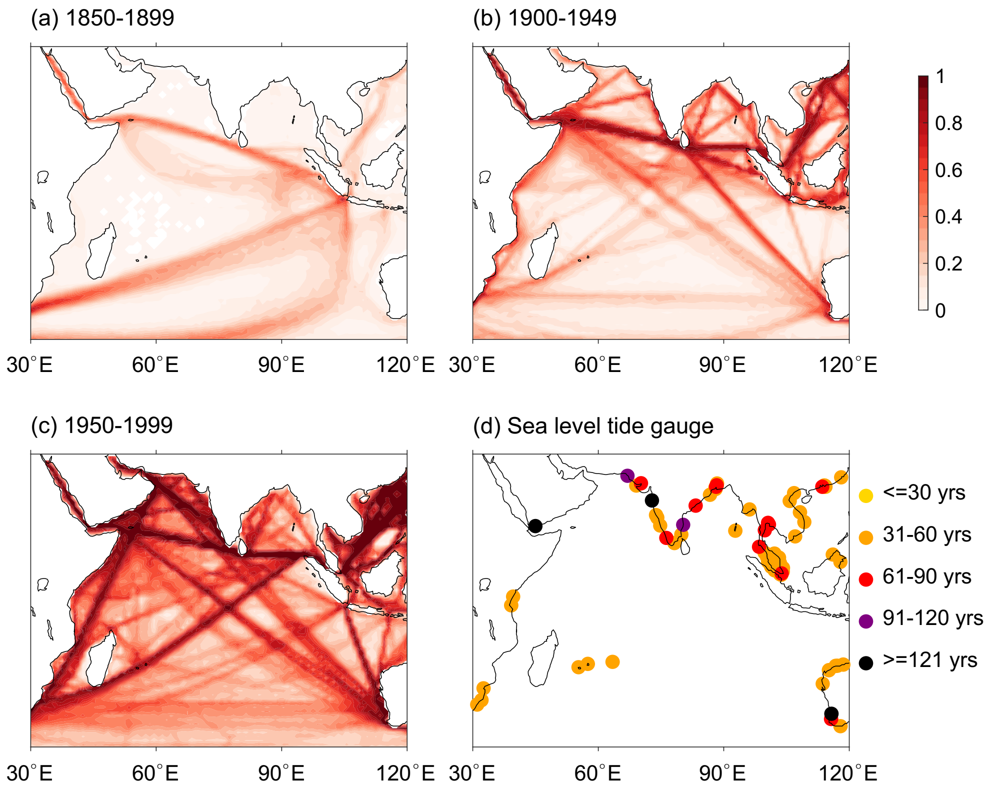

FIG. 1 (a)–(c) Distributions of sea surface temperature (SST) observations from HadSST2. Shown are the percentage of months with SST observations over the 50-year period. (d) Distribution of sea level tide gauges. Different colors represent different time length of available sea level data.

may introduce sampling errors, leading to significant uncertainties in studying decadal climate variability and long-term climate change signals based on instrumental climate datasets.

Instrumental biases. Instrumental measurements are not without biases or errors, which may even evolve over different time periods due to changing observational practices. In the 19th and early 20th centuries, SST was gauged by collecting water samples using uninsulated or partially insulated buckets from ships. From the middle of the 20th century, SST measurements transitioned to utilizing water intake from the engine room. This change in measurement techniques could lead to abrupt shifts in the SST record obtained from the same ships (Barnett, 1984), necessitating "correction" of the instrumental SST data. Since the late 1970s, global coverage satellite-derived SST data have become available. However, satellite measurements also carry biases, particularly due to the influence of aerosols and clouds. Additionally, unlike ships that measure bulk temperature, satellite observations capture skin temperature (Reynolds & Smith, 1994). These inconsistencies in SST measurements throughout the instrumental period add another layer of uncertainties when using the instrumental record for climate research, alongside the scarcity of observations in earlier periods.

Reconstructions. The presence of significant gaps and time-varying biases in the instrumental climate record introduce considerable uncertainties, restricting our ability to analyze Indian Ocean decadal climate variability. To address this, modern SST reconstructions employ "interpolation" techniques to fill gaps, especially in earlier periods, and "adjustment" or "correction" methods to mitigate the effects of the time-varying biases in the SST measurements (e.g., Nidheesh et al., 2017; Rayner et al., 2003). Similarly, sea level reconstructions combine large-scale sea level anomaly patterns associated with climate modes derived from satellite observations and tide gauge data to extend the observational record back in time (Church et al., 2004; Kumar et al., 2020). These products yield homogeneous gridded global SST and sea level data dating back to the mid-19th century. However, due to variations in the methods employed in different SST reconstructions and the scarcity of the raw data from the instrumental record for both SST and sea level datasets, significant cross-data differences persist (e.g., Nidheesh et al., 2017; Zhang et al., 2018b). Despite these efforts, uncertainties in the historical climate records continue to pose challenges in comprehensively understanding Indian Ocean decadal climate variability.

Uncertainties in Indian Ocean decadal variability and trends. The considerable uncertainties in the SST reconstructions present challenges in examining the decadal variability and long-term climate change in the Indian Ocean. In Fig. 2, we explore the decadal variability of the tropical Indian Ocean SST anomalies using empirical orthogonal function analysis of 8-year low-pass filtered monthly SST data spanning 1890 to 2015 from six different products. Overall, the filtered decadal variability explains 8% to 18% of the total variance in the six data sets. Before conducting the empirical orthogonal function analysis, the SST data were linearly interpolated onto uniform 2.5×2.5 degree grids, and the linear trend was removed to partly eliminate the influence of anthropogenic global warming. The first empirical orthogonal function mode (EOF1) reveals the main mode of decadal SST variability in the tropical Indian Ocean, characterized mainly by basin-scale SST anomalies of the same sign (Fig. 2a–f). As noted in prior studies, this behavior is primarily driven by the IPO through atmospheric teleconnections (Han et al., 2014). However, the six SST data sets clearly exhibit distinct SST anomaly patterns. Cobev2, HadISST, and Hurrell SST demonstrate maximum SST anomaly signals located in the central tropical Indian Ocean. In contrast, the 20CRv2c and ERSSTv4 datasets are associated with the strongest SST anomalies in the South Indian Ocean, especially near the so-called Seychelles-Chagos thermocline ridge (SCTR) or Seychelles Dome region, where the mean thermocline depth is shallow. ERA-20C, on the other hand, shows relatively weaker signals compared to other SST products, resulting in an explained variance of EOF1 of only 45%, smaller than others, which range roughly between 60% and 70%. These variations in SST anomaly patterns highlight the importance of accounting for data source differences when studying Indian Ocean decadal climate variability.

While the time evolution of the corresponding principal components (PC1) generally shows agreement across the six SST products, noticeable discrepancies arise during specific periods (Fig. 2g), particularly in the early 20th century, which is likely due to limited observations during that time. In recent decades, results from different SST products tend to converge, thanks to the advances in satellite observations that provide high-resolution global-scale SST measurements. In addition to uncertainties in internal decadal climate variability, long-term climate change signals also exhibit uncertainties to some extent (Fig. 2h). For instance, although all SST datasets indicate a relatively steady warming trend in the tropical Indian Ocean, there was a slowdown in the basin warming between the 1940s and 1960s. However, the magnitudes of the warming trend differ among the datasets. ERSSTv4 shows a warming trend of 0.74°C/century, whereas ERA-20C reflects a lower warming trend of 0.49°C/century. It is worth noting that such differences in warming trends may partly stem from uncertainties in internal climate variability. Consequently, both externally forced climate change signals (assessed by the linear trends) and internal decadal climate variability exhibit uncertainties across different SST reconstructions, posing challenges when investigating their associated mechanisms.

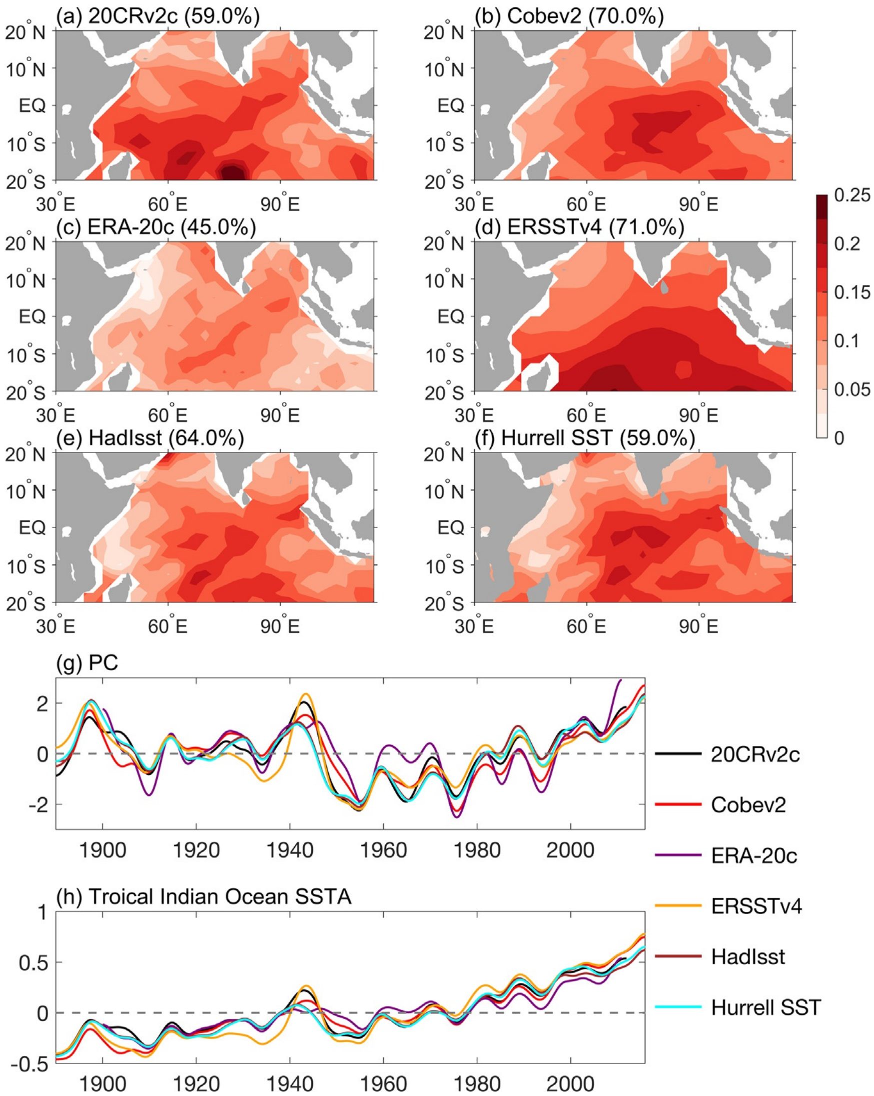

FIG. 2 (a)–(f) First Empirical Orthogonal Function (EOF1) mode of 8-year low-pass filtered SST anomalies in the tropical Indian Ocean from various SST data sets. Linear trend has been removed prior to the empirical orthogonal function analysis. Unit is °C. (g) Corresponding Principal Component (PC1). (h) 8-year lowpass filtered tropical Indian Ocean SST anomalies averaged in 30°E–120°E and 20°S–20°N. All SST data sets used here were interpolated into the same 2.5° by 2.5° grids.

3 Internal decadal climate variability

In comparison with the Pacific (e.g., Newman, 2016) and Atlantic (e.g., Liu, 2012), the exploration of decadal climate variations in the Indian Ocean has been relatively restricted. This section provides an overview of the existing literature that examines Indian Ocean decadal climate variability, addressing certain pertinent questions raised by a seminal review paper on this topic by Han et al. (2014).

3.1 Remote forcing from other regions

The decadal-to-interdecadal variability of SST in the tropical Indian Ocean has been observed to be in sync with the IPO as evidenced by instrumental records (Zhang et al., 1997) and proxy data (Cole et al., 2000). Until the 1960s, the SST variability of the tropical Indian Ocean was in phase with the IPO but a significant shift occurred after 1980, causing it to become out of phase with the Pacific SST variability (Zhang et al., 2018b). Observations and coupled climate model experiments suggest that this altered relationship can be primarily attributed to enhanced external forcing (Dong & McPhaden, 2017a; Zhang et al., 2018b). Zhang et al. (2018b) attributed this change to an earlier emergence of anthropogenic warming in the tropical Indian Ocean and volcanic eruptions in the 1980s and 1990s, leading to cooling over the region. In line with these findings, Dong and McPhaden (2017b) demonstrated that greenhouse gas forcing has contributed to warming the Indian Ocean, overpowering changes that would have arisen from the IPO, thereby weakening the dynamical links between the two ocean basins. Through coupled climate model experiments, it has been shown that in the absence of external forcing, the evolution of the Indian Ocean decadal variability would be considerably influenced by the IPO.

Numerous studies have emphasized the significance of the atmospheric bridge in shaping decadal variability. Copsey et al. (2006) attempted to simulate decadal sea level pressure (SLP) anomalies over the Indian Ocean using an atmospheric general circulation model but encountered difficulties in doing so. They proposed that remote forcing impacts atmospheric decadal variations in the Indian Ocean. To test this hypothesis, a recent study (Dong et al., 2016) used a coupled general circulation model and prescribed observed SST over the eastern tropical Pacific, predominantly influenced by the IPO on the decadal timescale This approach successfully reproduced observed decadal variations in the tropical Indian Ocean. Specifically, the IPO exerts a ~50% amplifying (or weakening) effect on the externally forced warming effect by ~50% during its warm (cold) phases. This indicates that the IPO influence via an atmospheric bridge plays an important role in the decadal SST variability of the tropical Indian Ocean. During a positive IPO phase, the Walker circulation weakens, resulting in anomalous descending motion over the tropical Indian Ocean. Consequently, there is reduced cloud cover and increased shortwave radiation reaching the ocean surface. Moreover, easterly wind stress anomalies over the equatorial Indian Ocean, associated with the weakened Walker circulation, trigger anomalous Ekman downwelling in off-equatorial regions. The combined effect of these processes leads to anomalous warming of the tropical Indian Ocean during a positive IPO. Importantly, these processes bear resemblance to the influence of the El Niño-Southern Oscillation (ENSO) on the Indian Ocean via the atmospheric bridge at interannual timescales (Alexander et al., 2002; Klein et al., 1999).

However, the above-mentioned decadal atmospheric bridge exhibits seasonal dependence. Han et al. (2017a) showed that the Walker circulations over the Pacific and Indian Oceans co-vary on the decadal timescale during boreal winter, primarily through fluctuations of atmospheric convection over the warm pool. In contrast, during boreal summer, the warm-pool convection only co-varies with the Pacific Walker circulation and not with the Indian Ocean Walker circulation. The latter is more strongly influenced by convective activity associated with the Indian summer monsoon, especially after the 1990s.

The role of the oceanic tunnel has also been under scrutiny. Dong and McPhaden (2016) found that an increase in heat transport by the ITF due to stronger trade winds during the recent hiatus period, associated with the negative IPO, led to enhanced warming in the Indian Ocean south of 10°S. A more comprehensive review of decadal sea level variability in the Indian Ocean due to the oceanic bridge from the Pacific can be found in Sprintall et al. (2024).

Both atmospheric bridge and oceanic tunnel from the IPO are suggested to influence interdecadal variations in the Ningaloo Niño, a climate mode characterized by positive SST anomalies off the west coast of Australia (Feng et al., 2013; Kataoka et al., 2014, 2017; Zhang et al., 2018a). Feng et al. (2015) and Li et al. (2017) showed that the occurrence of the Ningaloo Niño has increased since the late 1990s owing to the recent shift of the IPO to its negative phase. The enhanced ITF during the negative IPO is suggested to play a key role in this phenomenon. Furthermore, Tanuma and Tozuka (2020) revealed that the local positive feedback is intensified during the negative IPO phase, facilitated by the anomalously warm conditions to the northwest of Australia induced by the negative IPO phase through the atmospheric bridge (Li et al., 2019).

Decadal variability of sea level has also been observed over the Indian Ocean and shown to be enhanced during the 20th century along the coasts of global oceans (Little, 2023). Decadal variabilities of ENSO, Indian Ocean dipole (IOD), and monsoon largely account for the observed decadal sea level variability in different regions of the Indian Ocean (Han et al., 2018). Surface winds associated with these climate modes over the Indian Ocean are the main drivers for decadal sea level variability, while the Pacific influence via the ITF is strong mainly in the southeast basin.

3.2 Intrinsic Indian Ocean decadal variability

Ashok et al. (2004) proposed the existence of an intrinsic decadal climate mode known as the "decadal IOD," which is not correlated with decadal variability in the tropical Pacific and whose spatial pattern bears resemblance with the interannual IOD (Saji et al., 1999). Conversely, Tozuka et al. (2007) pointed out that decadal air-sea interactions associated with the "decadal IOD" may be a statistical artifact resulting from low-pass filtering. They suggested that it might emerge as an outcome of the decadal modulation of interannual IOD events or as a consequence of asymmetry in the occurrence of positive and negative IOD events. Additionally, they inferred that the decadal modulations in the interannual IOD are attributable to both intrinsic and remotely forced variability.

The Indian Ocean subtropical dipole is a dominant climate mode in the southern Indian Ocean (Behera & Yamagata, 2001; Reason, 2001). Positive (negative) SST anomalies are generated when the mixed layer becomes anomalously shallow (deep), with sensitivity to shortwave radiation being more (less) pronounced (Morioka et al., 2010). Yamagami and Tozuka (2015) conducted mixed-layer heat budget analyses, revealing that the thinner mixed layer in the recent decade amplifies this effect, making it possible for even weak atmospheric anomalies to trigger the Indian Ocean subtropical dipole. An examination of the Monin-Obukhov depth revealed an increasing trend in surface heat flux, attributed to decreased wind speeds (and increased specific humidity near the sea surface) linked to the poleward shift of the westerly jet in January (strengthening of the Mascarene High in February), resulting in a decreasing trend of the mixed layer depth. Regarding amplitude, Yan et al. (2013) demonstrated a weakening of the Indian Ocean subtropical dipole after 1979/80, although the exact mechanism behind this remains unknown. More recently, Zhang et al. (2022) highlighted a decadal eastward shift in the center of action for interannual climate modes, contributing to the recent weakening of the Indian Ocean subtropical dipole, while the amplitude of Ningaloo Niño has recently increased. Furthermore, based on an analysis of coupled model experiments, they proposed that internal climate variability plays a dominant role in these changes.

Li and Han (2015) conducted sensitivity experiments using an ocean general circulation model to investigate the mechanisms underlying decadal sea level variations in the Indian Ocean (Han et al., 2017b). This study revealed that the dominant mechanisms vary depending on the regions within the Indian Ocean. In most of the tropics, decadal modulations of wind stress anomalies associated with climate modes make a dominant contribution to sea level variations. However, off the Somali coast and the western Bay of Bengal, oceanic internal variability emerges as the primary driver. In the subtropical southern Indian Ocean, both surface heat flux and oceanic internal variability contribute, while stochastic winds become important in the southwest Indian Ocean, especially south of 30°S.

To assess the contribution of climate modes to decadal sea level variability in the Indian Ocean, Han et al. (2018) used a Bayesian dynamic linear model. Their study revealed that both decadal IOD and Indian monsoon surface wind variability play significant roles in regional decadal sea level variability, with some seasonal dependence. During boreal winter, both factors contribute to decadal variability to the northeast of Madagascar, while the Indian monsoon induces decadal variability off the Sumatra coast and along the Bay of Bengal coast. Conversely, in boreal summer, both decadal IOD and Indian monsoon influence decadal variability in the three aforementioned regions. For decadal sea level variability north of 5°S, the primary explanation may lie in the thermosteric sea level of the upper 700 m (Srinivasu et al., 2017) induced by decadal variations in surface winds over the Indian Ocean (Srinivasu et al., 2017; Thompson et al., 2016). Thompson et al. (2016) emphasized the importance of the cross-equatorial cell and deep equatorial upwelling, both influencing the upper ocean thermal distribution. The former is forced by zonal wind stress curl anomalies at the equator, and its decadal variability is associated with changes in the strength and position of the Mascarene High associated with the Indian Ocean subtropical dipole. However, Srinivasu et al. (2017) noted qualitative differences among different ocean reanalyzes in their finding.

Owing to the limited availability of sea level observational data over an extended period and inconsistencies among different ocean reanalysis products, Nidheesh et al. (2019) turned to control runs of phases 3 and 5 of the coupled model intercomparison project (CMIP) (Meehl et al., 2007; Taylor et al., 2012) to investigate decadal variations in sea level over the Indian Ocean. The leading mode of variability, explaining about 38% of the total variance on the decadal timescale, is associated with the decadal modulation of the IOD, which shows only a weak correlation with ENSO. During its positive phase, negative sea level anomalies occur in the eastern tropical Indian Ocean, with minima found along the Indonesian coast and west coast of Australia. Simultaneously, positive sea level anomalies are found in the western tropical Indian Ocean with a maximum located along 10°S. Conversely, the mode of variability, explaining around 14% of the variance, is characterized by positive sea level anomalies east of Madagascar. The mechanism driving this mode is model dependent. In some models, downwelling Rossby waves induced by anticyclonic wind stress anomalies in the southeastern tropical Indian Ocean (Nidheesh et al., 2013) associated with the meridional shift of the Mascarene High contribute to this mode. In other models, positive sea level anomalies induced by alongshore wind stress anomalies off the west coast of Australia are radiated away from the coast as westward propagating Rossby waves and also play a role. Zhuang et al. (2013) highlighted the importance of wind stress curl anomalies in the region of 70°E–95°E for triggering the Rossby waves, using a baroclinic Rossby wave model. Additionally, Zhang et al. (2019) demonstrated that the meridional shift in the Mascarene High, which is uncorrelated with ENSO, contributes to the generation of sea level anomalies east of Madagascar, emphasizing the importance of intrinsic Indian Ocean variability.

4 Externally forced signals

4.1 Detection and attribution of Indian Ocean warming

Over recent decades, the Indian Ocean has undergone a rapid basin-wide warming trend, exceeding that of other tropical oceans (Han et al., 2014; Luo et al., 2012). Despite being detectable amidst background "climate noise" (Gopika et al., 2020), the underlying cause of this warming remains a topic of debate. The Indian Ocean warming in observations is likely the result of external forcing, particularly greenhouse gas forcing (Alory et al., 2007; Barnett et al., 2005; Dong et al., 2014; Dong & Zhou, 2014; Knutson, 2006; Pierce et al., 2006; Roxy et al., 2020). To evaluate the exact contributions of greenhouse gases and anthropogenic aerosols, including direct and indirect aerosol effects, to the Indian Ocean warming, the CMIP protocol encouraged simulations encompassing all forcing, greenhouse gas-only forcing, natural-only forcing simulations, and anthropogenic aerosol-only forcing.

Fig. 3 compares the time evolution from the basin-averaged warming in observations and the multimodel ensemble averages of different forcings. A significant warming trend during 1870–2005 is evident in the observations, particularly rapid in the latter half of the 20th century (Fig. 3a). This warming trend is well reproduced by all forcing runs (Fig. 3b). Greenhouse gas forcing exerts the dominant role on the Indian Ocean warming trend, with a persistent warming effect throughout the 20th century (Fig. 3c). In contrast, the total anthropogenic aerosols effect (including both direct and indirect effects) cools the basin-averaged SST and slows down the warming trend (Fig. 3d). The direct aerosol effect reduces shortwave radiation reaching the Earth's surface by absorbing or scattering the sunlight, while the indirect effect of aerosols affects surface radiative flux through its influence on clouds. Notably, the cooling was more pronounced after the 1950s due to the increased emission of anthropogenic aerosols with postwar economic growth (Xie et al., 2013). However, when considering only the direct effect of aerosols, the cooling effect is weakened (Fig. 3e), although the SST anomaly signals may still contain natural decadal variability due to the limited number of ensemble members. The observed trend of 0.40 K century^{-1} closely aligns with all forcing runs of 0.41 ± 0.16 K century^{-1} (standard deviation of intermodel variations). Under greenhouse gas-only forcing, the warming trend is stronger than in observations and the all forcing run (0.66 ± 0.14 K century^{-1}). For each of the 17 CMIP5 models, the warming trend under greenhouse gas forcing is positive

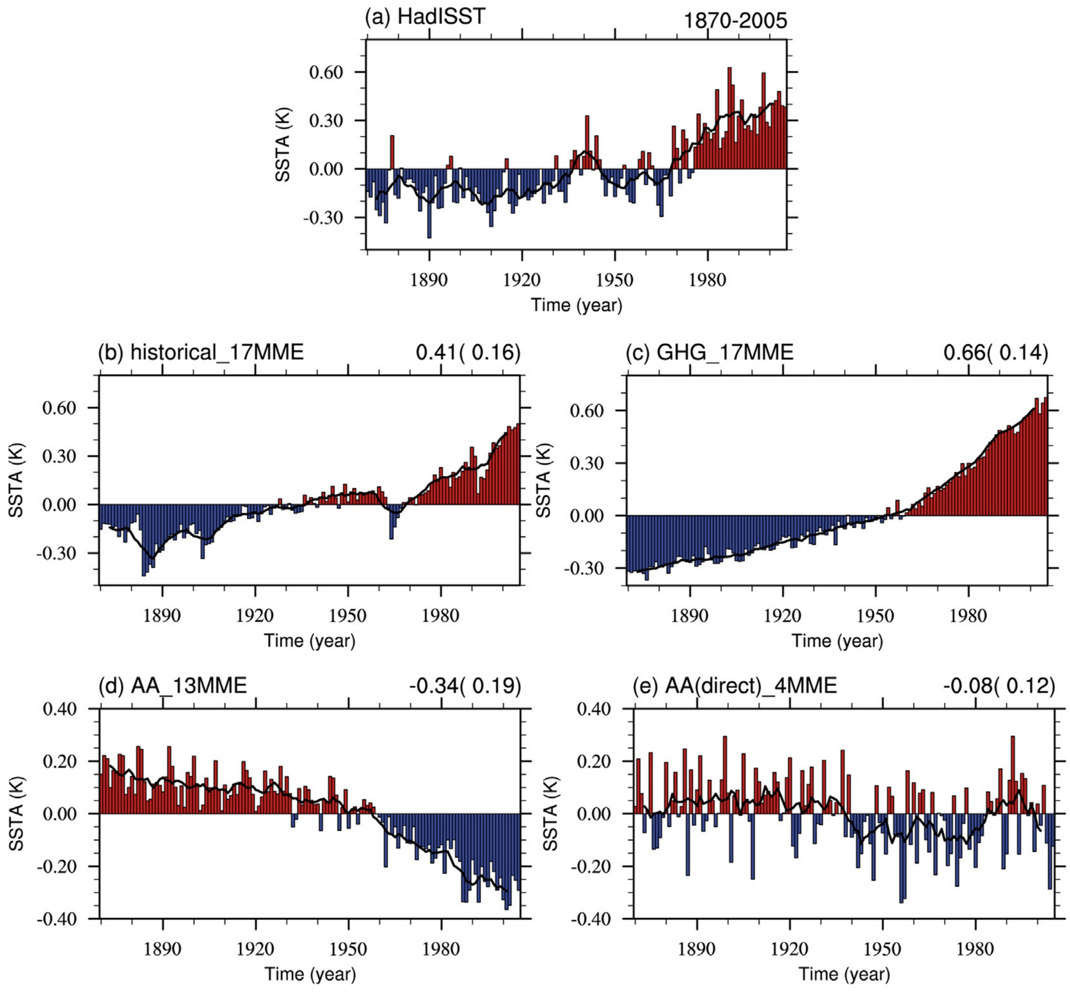

FIG. 3 Time series of Indian Ocean (40°S–15°N, 40°–100°E) annual mean (bar) and 8-yr running average (line) sea surface temperature anomaly (SSTA) from (a) observations, (b) all forcing runs of 17 models from the multimodel ensemble (MME), (c) Greenhouse gas (GHG)-only forcing runs of 17 models of the MME, (d) Anthropogenic aerosols (AA)-only forcing of 13 models from the MME that include both direct and indirect effects, and (e) AA-only forcing of four models from the MME that only include direct effects. Only one member is used for each model. SSTA is relative to the period of 1870–2005 mean. Units: K. The numbers on the top right of (b)–(e) denote the trend values and standard deviation of intermodel variations (in K century^{-1}), respectively. *(From Dong and Zhou (2014). © American Meteorological Society. Used with permission.)*

with the multimodel ensemble mean accounting for about 163.6%. In contrast, the emission of anthropogenic aerosols has mitigated the warming trend, with negative contributions to the warming, except for CCSM4, which exhibits weak warming. Based on the result of the multimodel ensemble mean, anthropogenic aerosols reduce the warming trend of all forcing runs by 72.7%. If only the direct effect of aerosols is considered, there is a weak cooling trend of -0.08 ± 0.12 K century^{-1} (Fig. 3e). However, when including both direct and indirect effects, the cooling trend is enhanced to -0.34 ± 0.19 K century^{-1} (Fig. 3d), offsetting roughly half of greenhouse gas warming. Consequently, the warming rate of the Indian Ocean, though faster than the global mean, reflects the competing influences of greenhouse gases and anthropogenic aerosols on the Indian Ocean SST changes, akin to their effects on global mean SST (Han et al., 2014).

Apart from the centennial and multidecadal warming trends, the Indian Ocean SST also exhibits decadal-to-interdecadal variability (Fig. 3) arising from both internal climate variability (Section 3) and external forcing. As discussed in Section 3, strong external forcing weakens the dynamical connection between the Indian and Pacific Oceans, resulting in the inability of the negative phase of the IPO after 2000 to induce a cold SST anomaly over the Indian Ocean in observations (Dong & McPhaden, 2017a). This enhanced external forcing after the 1980s can be primarily attributed to greenhouse gases, with anthropogenic aerosol forcing and natural forcing exhibiting relatively weak impacts (Dong & McPhaden, 2017b).

4.2 Nonuniform warming patterns

The Indian Ocean basin-averaged SST displays a robust warming trend, yet this warming is spatially heterogeneous, exhibiting an uneven warming pattern. Understanding this pattern is crucial for comprehending the global climate response to increasing greenhouse gases. For instance, this SST warming pattern strongly constrains the regional distribution of precipitation changes over the tropical ocean, following a warmer-get-wetter mechanism (Grose et al., 2014; Kent et al., 2015; Kosaka & Xie, 2016; Xie et al., 2010). Additionally, the pattern of tropical SST change can influence large-scale circulation in the tropical atmosphere, exerting a notable impact on extratropical climates (Lee et al., 2022; Trenberth et al., 1998) such as in the North Atlantic and Arctic regions (Hoerling et al., 2004; Hu & Fedorov, 2020; Xu et al., 2022). Consequently, detecting the spatial warming pattern in the Indian Ocean and exploring the associated mechanisms are of utmost importance.

Attribution of spatial patterns. Fig. 4 illustrates the pattern of SST trend in the Indian Ocean during 1870–2005 based on observations and multimodel ensemble simulations with various external forcings. Observations display basin-wide warming trends over the past century, with the most substantial warming observed in the western tropical Indian Ocean and relatively weaker warming in the tropical south Indian Ocean, resembling the positive IOD-like SST pattern (Cai et al., 2013; Du & Xie, 2008; Roxy et al., 2014; Xie et al., 2010; Zheng et al., 2010; see Fig. 4a). Externally forced enhanced warming in the Arabian Sea and western tropical Indian Ocean relative to the rest of the basin simulated by CMIP models is already detectable, which aligns with observations. The multimodel ensemble mean of all forcing runs captures a significant portion of the observed east-west dipole warming pattern (Fig. 4a and b), predominantly due to greenhouse gas forcing (Fig. 4c). This pattern weakens the Walker cell, leading to easterly wind anomalies in the equatorial Indian Ocean and consequently the positive IOD-like warming pattern (Cai et al., 2013). However, observational analyses present conflicting views on the Walker cell changes in recent decades (Han et al., 2014). In contrast, direct anthropogenic aerosol forcing results in a weak but opposite SST change pattern, counteracting the effect of greenhouse gas warming (Fig. 4e). The total (direct and indirect) aerosol forcing yields stronger cooling in the north Indian Ocean and comparatively less cooling in the subtropical south Indian Ocean (Fig. 4c and d). Moreover, the warming (cooling) rate in response to greenhouse gas (anthropogenic aerosol) forcing is more pronounced in the northern basin than in the southern basin (Fig. 4c and d). The stronger cooling effect from anthropogenic aerosol in the northern basin may be attributed to the presence of anthropogenic aerosols originating from Asia.

Mechanisms. The mechanism underlying the Indian Ocean response to the greenhouse gas forcing remains a subject of investigation in climate models (Du & Xie, 2008). Some studies suggested that basin-wide SST warming is directly triggered by atmospheric processes, initiated by the increase in downward longwave radiation due to greenhouse gases, and then amplified by the water vapor feedback and atmospheric adjustment in climate models (Du & Xie, 2008). On the other hand, other studies suggest a link between this SST change and changes in ocean heat transport. For example, Indian Ocean basin-wide warming is associated with ocean wave-induced thermocline changes (Li et al., 2003) or a decrease in upwelling related to a slowdown of the wind-driven Ekman pumping (Alory & Meyers, 2009). Few modeling studies have indicated contributions from both atmospheric and oceanic processes. Ocean temperature advection is regarded as the dominant process for the increase of the northern Indian Ocean heat content, whereas control by surface heat fluxes prevails in other areas of the Indian Ocean basin (Barnett et al., 2005).

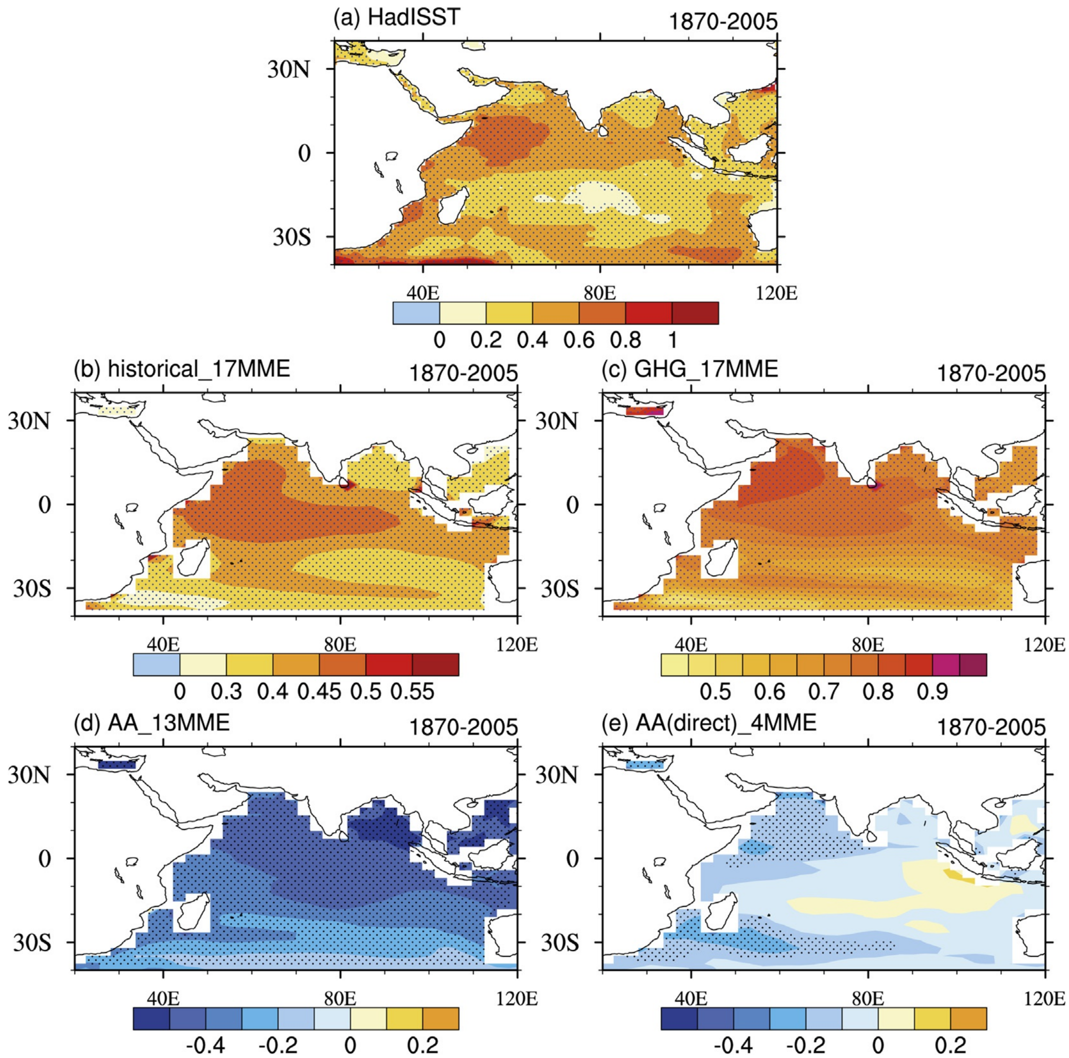

FIG. 4 Trends of SST in the Indian Ocean during 1870–2005 from (a) observations, (b) all forcing runs of a 17-model multimodel ensemble (MME), (c) Greenhouse gas (GHG)-only forcing runs of a 17-model MME, (d) Anthropogenic aerosol (AA)-only forcing of a 13-model MME, and (e) direct effects of AA-only forcing of a 4-model MME. The dotted areas are statistically significant at the 1% level by Student's *t*-test. Note that the color scale intervals are not the same for each figure. Units: K $(100\,\mathrm{year})^{-1}$. *(From Dong and Zhou (2014). © American Meteorological Society. Used with permission.)*

Water cycle. As for SST, the observed sea surface salinity (SSS) trend patterns from 1950 to 2019 are reasonably captured by the multimodel ensemble mean of CMIP6 simulations, albeit an underestimated amplitude (Fig. 5). Both the observed and simulated SSS changes generally enhance the mean SSS patterns, resulting in fresher conditions in the Bay of Bengal and equatorial basin, where mean salinity is low and precipitation (P) exceeds evaporation (E) (E-$P<0$), and saltier conditions in the subtropical south Indian Ocean, where mean salinity is high and E-$P>0$. These findings suggest an intensified water cycle driven by greenhouse gas forcing (Durack, 2015; Eyring et al., 2021), with an 8% pattern amplification for E-P change, which is close to the 7% increase in tropospheric relative humidity, corresponding to each degree of global surface warming (Douville et al., 2022; Durack et al., 2012). Projections from climate models indicate that this pattern of amplification of SSS is expected to increase by the end of the 21st century.

Sea level trends. Distinct spatial patterns of sea level trend since the 1950s have been identified after removing the global mean sea level rise, showing regional sea level fall in the southwest tropical Indian Ocean and rise in the eastern Indian Ocean (Fig. 6a–d; Dunne et al., 2012; Han, 2010; Han et al., 2018; Schwarzkopf & Böning, 2011; Timmermann et al., 2010). While thermosteric sea level dominates the upper 2000m total steric sea level trends for the 1950–2008 period in most regions of the Indian Ocean, halosteric changes associated with the water cycle can be the leading

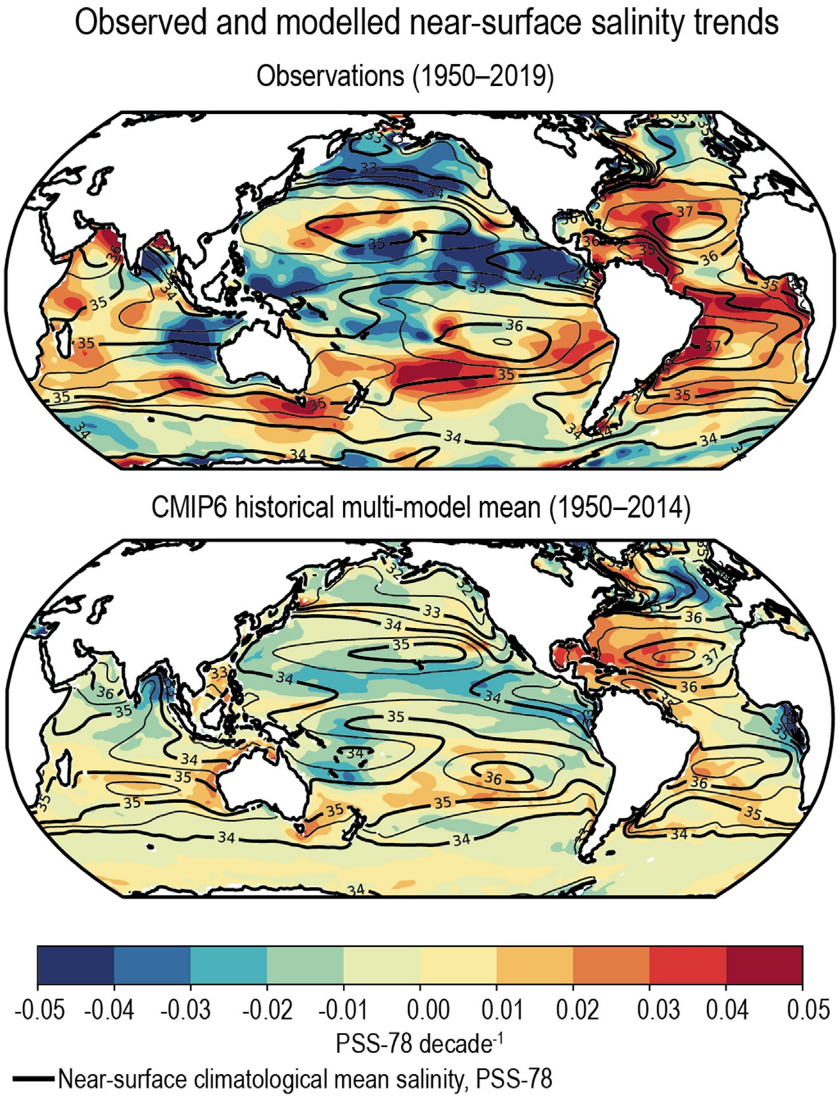

FIG. 5 Multidecadal salinity trends for the near-surface ocean (in Practical Salinity Scale 1978 [PSS-78] per decade). *(Top)* Observed trend. *(Bottom)* Simulated trend from the CMIP6 historical experiment multimodel mean (1950–2014). Black contours show the climatological mean salinity in increments of 0.5 PSS-78 (thick lines 1 PSS-78). *(From Eyring et al. (2021).)*

contributor to total steric changes in the tropical southeast Indian Ocean and subtropical South Indian Ocean (Durack et al., 2012). Indeed, the importance of salinity in causing positive sea level trends in the tropical southeast Indian Ocean for the 2005–2013 decade has also been shown, due to enhanced precipitation in the maritime continent region and strengthened ITF (Llovel & Lee, 2015). In addition, halosteric sea level shows large-scale decreasing trends due to increased salinity in the North Indian Ocean (10°S–20°N) and increasing trends due to decreased salinity in the South Indian Ocean (30°S–10°S) for the 2005–2015 period. Trend patterns of dynamical sea level (global mean removed) from large ensemble experiments using two global climate models bear some resemblance with the observed patterns, particularly the sea level fall in the southwest basin (Fig. 6e–h). This relative decline was primarily attributed to internal climate variability with external forcing contributing ~19% ± 2.4% (Han et al., 2018). However, significant qualitative and quantitative differences exist between the two climate model simulations in most regions of the Indian Ocean, introducing considerable uncertainty in the climate model's ability to simulate the forced signals of regional sea level changes.

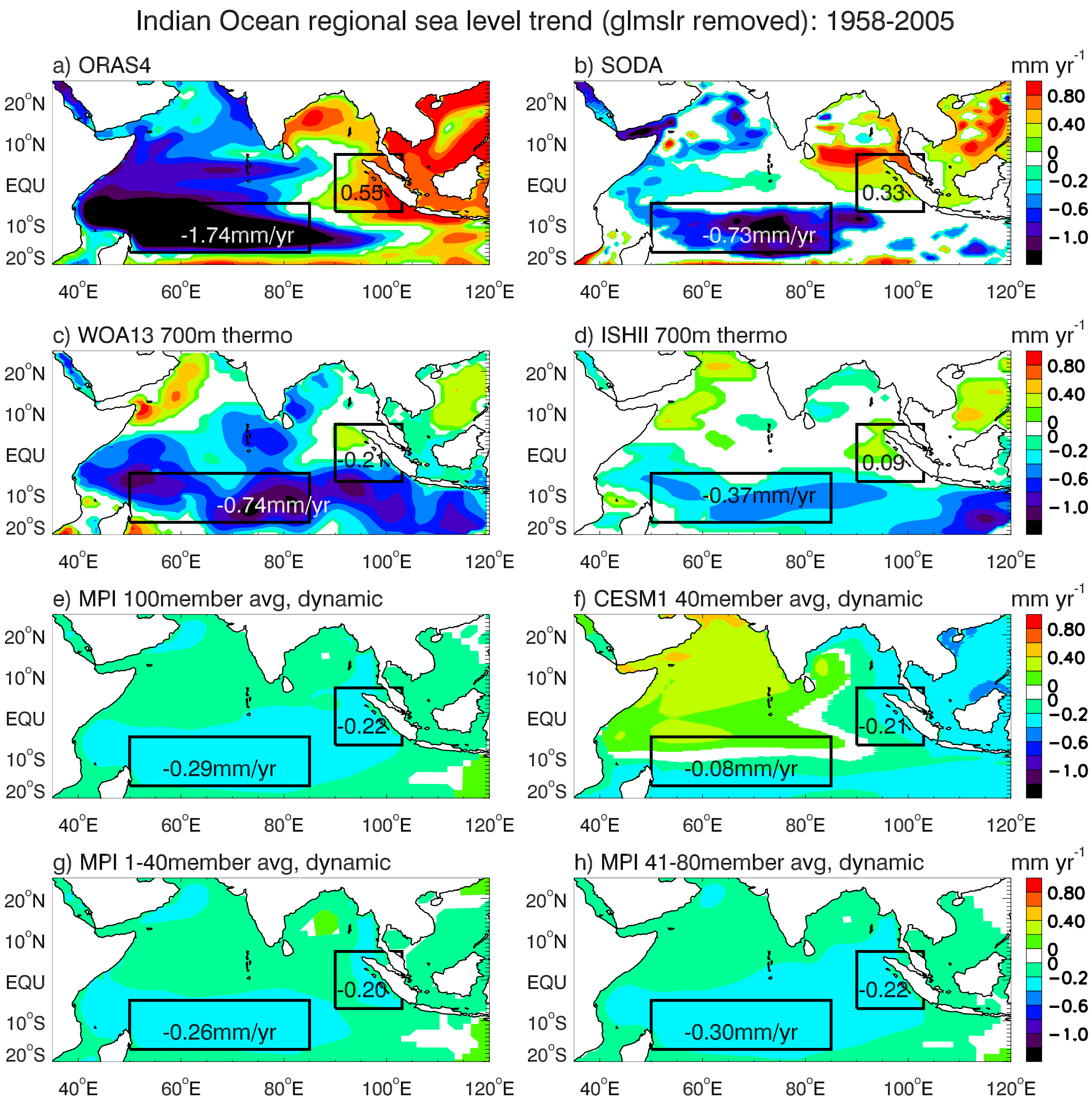

FIG. 6 The linear trends of regional sea level over the tropical Indian Ocean from 1958 to 2005. Monthly data are used, with the 1958–2005 monthly climatology and global mean sea level rise time series removed from each dataset before the trend calculation. (a) The ECMWF Ocean Reanalysis System 4 (ORAS4) reanalysis; (b) the Simple Ocean Data Assimilation (SODA) reanalysis; (c) the world ocean atlas 2013 (WOA13) upper 700 m thermosteric sea level; (d) Ishii upper 700 m thermosteric sea level; (e) the Max-Planck-Institute of Meteorology (MPI) 100-member ensemble mean dynamic sea level; (f) the National Center for Atmospheric Research (NCAR) community earth system model version 1 (CESM1) 40-member ensemble mean dynamic sea level; (g) MPI ensemble mean for members 1–40; (h) MPI ensemble mean for members 41–80. The two boxes show the maximum sea level fall and rise areas in both the ORAS4 and SODA dynamic sea level, with Reg. 1 located in the thermocline ridge of the southwest tropical basin (50° E–85° E, 17° S–5° S) and Reg. 2, eastern equatorial Indian Ocean (90° E–103° E, 7° S–7° N). The number in each box shows the trend value of SLA averaged in the box. Trend values exceeding 95% significance are shown in color contours, and those below 95% are shown in white. *(From Han et al. (2018).)*

5 Predictability

Earlier CMIP (CMIP3 and before) have demonstrated that near-term climate predictions, ranging between 2 and 30 years, were influenced by a combination of external forcing and internal variability (Doblas-Reyes et al., 2013). However, to bridge the gap between subseasonal-to-seasonal predictions and climate projections, the focus has shifted to decadal predictions, which have become a prominent area of research since CMIP5 (Doblas-Reyes et al., 2013; Kirtman et al., 2013). Coordinated experiments, as conducted in CMIP5, have explored the potential of initializing coupled models with observational data. This initialization allows for the prediction of internal variability in addition to changes associated with external forcing, offering valuable insights into decadal climate trends (Doblas-Reyes et al., 2013; Kirtman et al., 2013; Smith et al., 2007).

The Indian Ocean stands out as the region with the highest decadal prediction skill for SST over the global ocean in 2–9 years lead forecasts. Guemas et al. (2013) demonstrated that anomaly correlation coefficients of SST anomalies averaged over the Indian Ocean (40°S–30°N, 20°–120°E) remain consistently high at 0.7 for 2–9 years lead forecasts, surpassing other basins. This enhanced prediction skill can be attributed to the predominance of varying radiative forcings linked to increasing anthropogenic greenhouse gases and volcanic aerosols, which exert a stronger influence than relatively weak internal variability. Interestingly, initializing coupled models with observed climate states did not lead to significant skill improvements in the Indian Ocean due to the dominance of external forces. This is in stark contrast with other basins, where natural decadal climate variability plays a more significant role. However, in the western Indian Ocean, multimodel decadal SST predictions from the CMIP5 models indicate some improvements with initialization, even though SLP forecasts deteriorate (Smith et al., 2019). This contrasting impact of initialization on SST and SLP suggests potential issues in the representation of ocean-atmosphere interaction over the western Indian Ocean or the involvement of different mechanisms governing their predictability. Morioka et al. (2018) conducted a study on decadal climate variability in the southern Indian Ocean. They found that observed decadal SST variations were particularly large east of Madagascar, off the west coast of Australia, and in the Agulhas Return Current region. Furthermore, their coupled model demonstrated relatively high skill in the Agulhas Return Current region for a lead time of up to 9 years. They suggested that this enhanced predictability may be attributed to the model's successful representation of eastward propagation of anomalously warm SST coupled with positive SLP anomalies from the Atlantic and local air-sea interactions.

6 Conclusions

In Section 3, our review has highlighted recent advancements in understanding decadal climate variability in the Indian Ocean, arising from both remote forcing from other basins and intrinsic processes. Remote forcing, particularly from the IPO, exerts its influence through both the atmospheric bridge and oceanic tunnel, with the Walker circulation and the ITF playing key roles. However, the relative contributions of these effects still require further quantification, and improved coupled general circulation models are needed to realistically simulate interbasin interactions. Regarding intrinsic variability, research has explored how interannual climate modes like IOD and Indian Ocean subtropical dipole vary on decadal timescales. Yet, there is a need for more in-depth investigations to fully uncover the underlying mechanisms. One intriguing question that warrants future exploration is the potential role of reemergence in decadal climate variability, particularly in the subtropical southern Indian Ocean. Reemergence is a process by which wintertime SST anomalies that extend throughout a deep mixed layer are preserved beneath the thin summer mixed layer after the mixed layer shoals, but when the mixed layer becomes deeper again in the subsequent autumn and winter, subsurface water with temperature anomalies is re-entrained into the mixed layer and SST anomalies with the same sign recur. While reemergence has been implicated in the PDO (Newman, 2016), its significance in the Indian Ocean remains relatively unexplored.

In summary of Section 4, our understanding of externally forced signals in the Indian Ocean heavily relies on multimodel ensemble analyses. We have quantitatively compared the relative contributions of greenhouse gases and anthropogenic aerosols, revealing greenhouse gases as the dominant factor driving rapid warming and anthropogenic aerosols mitigating the warming rate. The mechanisms governing the basin-wide warming pattern have been attributed to atmospheric processes involving radiative and turbulent fluxes, while the positive IOD-like warming pattern is closely related to the surface wind anomalies. Nonetheless, uncertainties persist in climate model simulations, warranting further investigation into the relative impact of model biases and internal variability in reproducing and projecting the multidecadal warming, sea level, and SSS spatial patterns. Quantifying and understanding these uncertainties are vital for providing informed and reliable projections of future changes.

In Section 5, we delved into decadal predictions in the Indian Ocean, where SST prediction skill is notably high, primarily driven by varying radiative forcings linked to anthropogenic greenhouse gases and volcanic aerosols. However, our ability to predict internal variability on decadal time scales remains limited and requires further advancements.

As stated in the introduction, a crucial motivation for understanding decadal variations in the Indian Ocean is its potential role in the global warming hiatus. While the extra heat absorbed by the tropical Pacific is largely transported to the Indian Ocean via the ITF (Lee et al., 2015; Nieves et al., 2015; Zhang et al., 2018b), the ultimate fate of this heat is still uncertain. Unraveling whether the extra heat is released back into the atmosphere within the Indian Ocean or transported southward to the Southern Ocean (Vialard, 2015) remains an outstanding question. Both observational data analyses and model studies are necessary to address this important issue in the coming decade.

Although Section 2 has reviewed the continued efforts in observing the Indian Ocean (Beal et al., 2020; Hermes et al., 2019), historical observational datasets still exhibit large uncertainties, particularly in earlier periods. Hence, establishing a sustained observational system in the Indian Ocean is essential to extend data coverage with improved quality and enhance our understanding of its decadal climate variability. The IndOOS initiative, as detailed in McPhaden et al. (2024), plays a critical role in this endeavor, and incorporating subsurface observations can further enhance our understanding of decadal variations in the Indian Ocean, including the fate of extra heat stored in the Indian Ocean during the recent hiatus in global warming.

7 Educational resources

- The Decadal Climate Prediction Project of the World Climate Research Programme (WCRP) (https://www.wcrp-climate.org/dcp-overview).
- WCRP Grand Challenge on Near-Term Climate Prediction (https://www.wcrp-climate.org/gc-near-term-climate-prediction).

Acknowledgments

We sincerely thank two reviewers, Mike McPhaden and Tangdong Qu, for their constructive comments and suggestions that helped us greatly to improve our book chapter. WH is supported by NSF AGS 1935279 and NSF OCE 2242193.

Author contributions

For the first draft, TT wrote Sections 1, 3, 5, and 6, LZ wrote Section 2, and LD and WH wrote Section 4. ML contributed to the writing of all sections. All authors read and approved the final manuscript.

References

Alexander, M. A., Bladé, I., Newman, M., Lanzante, J. R., Lau, N.-C., & Scott, J. D. (2002). The atmospheric bridge: The influence of ENSO teleconnections on air–sea interaction over the global oceans. *Journal of Climate*, *15*, 2205–2231.

Alory, G., & Meyers, G. (2009). Warming of the upper equatorial Indian Ocean and changes in the heat budget (1960–99). *Journal of Climate*, *22*, 93–113.

Alory, G., Wijffels, S., & Meyers, G. (2007). Observed temperature trends in the Indian Ocean over 1960–1999 and associated mechanisms. *Geophysical Research Letters*, *34*, L02606.

Al-Yamani, F. Y., Burt, J. A., Goes, J. I., Jones, B., Nagappa, R., Murty, V. S. N., … Yamamoto, T. (2024). Chapter 16: Physical and biogeochemical characteristics of the Indian Ocean marginal seas. In C. C. Ummenhofer, & R. R. Hood (Eds.), *The Indian Ocean and its role in the global climate system* (pp. 365–391). Amsterdam: Elsevier. https://doi.org/10.1016/B978-0-12-822698-8.00008-1.

Ashok, K., Chan, W.-L., Motoi, T., & Yamagata, T. (2004). Decadal variability of the Indian Ocean dipole. *Geophysical Research Letters*, *31*, L24207.

Barnett, T. P. (1984). Long-term trends in surface temperature over the oceans. *Monthly Weather Review*, *112*, 303–312.

Barnett, T. P., Pierce, D. W., AchutaRao, K. M., Gleckler, P. J., Santer, B. D., Gregory, J. M., & Washington, W. M. (2005). Penetration of human-induced warming into the world's oceans. *Science*, *309*, 284–287.

Beal, L., et al. (2020). A roadmap to IndOOS-2: Better observations of the rapidly-warming Indian Ocean. *Bulletin of the American Meteorological Society*, *101*, E1891–E1913.

Behera, S. K., & Yamagata, T. (2001). Subtropical SST dipole events in the southern Indian Ocean. *Geophysical Research Letters*, *28*, 327–330.

Cai, W., Zheng, X., Weller, E., Collins, M., Cowan, T., Lengaigne, M., Yu, W., & Yamagata, T. (2013). Projected response of the Indian Ocean dipole to greenhouse warming. *Nature Geoscience*, *6*, 999–1007.

Church, J. A., White, N. J., Coleman, R., Layback, K., & Mitrovica, J. X. (2004). Estimates of the regional distribution of sea level rise over the 1950–2000 period. *Journal of Climate*, *17*, 2609–2625.

Cole, J. E., Dunbar, R. B., McClanahan, T. R., & Muthiga, N. A. (2000). Tropical Pacific forcing of decadal SST variability in the western Indian Ocean over the past two centuries. *Science*, *287*, 617–619.

Copsey, D., Sutton, R., & Knight, J. R. (2006). Recent trends in sea level pressure in the Indian Ocean region. *Geophysical Research Letters*, *33*, L19712.

Doblas-Reyes, F. J., Andreu-Burillo, I., Chikamoto, Y., García-Sarrano, J., Guemas, V., Kimoto, M., Mochizuki, T., Rodrigues, L. R. L., & van Oldenborgh, G. J. (2013). Initialized near-term regional climate change prediction. *Nature Communications*, *4*, 1715.

Dong, L., & McPhaden, M. J. (2016). Interhemispheric SST gradient trends in the Indian Ocean prior to and during the recent global warming hiatus. *Journal of Climate*, *29*, 9077–9095.

Dong, L., & McPhaden, M. J. (2017a). Why has the relationship between Indian and Pacific Ocean decadal variability changed in recent decades? *Journal of Climate*, *30*, 1971–1983.

Dong, L., & McPhaden, M. J. (2017b). The effects of external forcing and internal variability of the formation of interhemispheric sea surface temperature gradient trends in the Indian Ocean. *Journal of Climate*, *30*, 9077–9095.

Dong, L., & Zhou, T. J. (2014). The Indian Ocean Sea surface temperature warming simulated by CMIP5 models during the twentieth century: Competing forcing roles of GHGs and anthropogenic aerosols. *Journal of Climate*, *27*, 3348–3362.

Dong, L., Zhou, T. J., Dai, A., Song, F. F., Wu, B., & Chen, X. L. (2016). The footprint of the inter-decadal Pacific oscillation in Indian Ocean Sea surface temperatures. *Scientific Reports*, *6*, 21251.

Dong, L., Zhou, T. J., & Wu, B. (2014). Indian Ocean warming during 1958–2004 simulated by a climate system model and its mechanism. *Climate Dynamics*, *42*, 203–217.

Douville, H., Qasmi, S., Ribes, A., & Bock, O. (2022). Global warming at near-constant tropospheric relative humidity is supported by observations. *Communications Earth & Environment*, *3*, 237.

Du, Y., & Xie, S.-P. (2008). Role of atmospheric adjustments in the tropical Indian Ocean warming during the 20th century in climate models. *Geophysical Research Letters*, *35*, L08712.

Dunne, R. P., Barbosa, S. M., & Woodworth, P. L. (2012). Contemporary sea level in the Chagos Archipelago, Central Indian Ocean. *Global and Planetary Change*, *82–83*, 25–37.

Durack, P. J. (2015). Ocean salinity and the global water cycle. *Oceanography*, *28*, 20–31.

Durack, P. J., Wijffels, S. E., & Matear, R. J. (2012). Ocean salinities reveal strong global water cycle intensification during 1950–2000. *Science*, *336*, 455–458.

England, M. H., et al. (2014). Recent intensification of wind-driven circulation in the Pacific and the ongoing warming hiatus. *Nature Climate Change*, *4*, 222–227.

Eyring, V., Gillett, N. P., Achuta Rao, K. M., Barimalala, R., Barreiro Parrillo, M., Bellouin, N., Cassou, C., Durack, P. J., Kosaka, Y., McGregor, S., Min, S., Morgenstern, O., & Sun, Y. (2021). Human influence on the climate system. In V. Masson-Delmotte, P. Zhai, A. Pirani, S. L. Connors, C. Péan, S. Berger, N. Caud, Y. Chen, L. Goldfarb, M. I. Gomis, M. Huang, K. Leitzell, E. Lonnoy, J. B. R. Matthews, T. K. Maycock, T. Waterfield, O. Yelekçi, R. Yu, & B. Zhou (Eds.), Climate change 2021: The physical science basis. Contribution of working group I to the sixth assessment report of the intergovernmental panel on climate change. Cambridge, United Kingdom and New York, NY: Cambridge University Press, pp. 423–552. https://doi.org/10.1017/9781009157896.005. Chapter 3.

Feng, M., Hendon, H. H., Xie, S.-P., Marshall, A. G., Schiller, A., Kosaka, Y., Caputi, N., & Pearce, A. (2015). Decadal increase in Ningaloo Niño since the late 1990s. *Geophysical Research Letters*, *42*, 104–112.

Feng, M., McPhaden, M. J., Xie, S.-. P., & Hafner, J. (2013). La Niña forces unprecedented Leeuwin current warming in 2011. *Scientific Reports*, *3*, 1277.

Gopika, S., Izumo, T., Vialard, J., Lengaigne, M., Suresh, I., & Kumar, M. R. R. (2020). Aliasing of the Indian Ocean externally-forced warming spatial pattern by internal climate variability. *Climate Dynamics*, *54*, 1093–1111.

Grose, M. R., Bhend, J., Narsey, S., Gupta, A. S., & Brown, J. R. (2014). Can we constrain CMIP5 rainfall projections in the tropical Pacific based on surface warming patterns? *Journal of Climate*, *27*, 9123–9138.

Guemas, V., Corti, S., García-Serrano, J., Doblas-Reyes, F. J., Balmaseda, M., & Magnusson, L. (2013). The Indian Ocean: The region of highest skill worldwide in decadal climate prediction. *Journal of Climate*, *26*, 726–739.

Hamlington, B. D., Strassburg, M. W., Leben, R. R., Han, W., Nerem, R. S., & Kim, K.-Y. (2014). Uncovering an anthropogenic sea-level rise signal in the Pacific Ocean. *Nature Climate Change*, *4*, 782–785.

Han, W., Meehl, G. A., Hu, A., Zheng, J., Kenigson, J., Vialard, J., … Yanto. (2017a). Decadal variability of Indian and Pacific Walker cells: Do they co-vary on decadal timescales? *Journal of Climate*, *30*, 8447–8468.

Han, W., Meehl, G., Stammer, D., Hu, A., Hamlington, B., Kenigson, J., … Thompson, P. (2017b). Spatial patterns of sea level variability associated with natural internal climate modes. *Surveys in Geophysics*, *38*, 217–250.

Han, W., Stammer, D., Meehl, G. A., Hu, A., Sienz, F., & Zhang, L. (2018). Multi-decadal trend and decadal variability of the regional sea level over the Indian Ocean since the 1960s: Roles of climate modes and external forcing. *Climate*, *6*, 51.

Han, W., Vialard, J., McPhaden, M. J., Lee, T., Masumoto, Y., Feng, M., & de Ruijter, W. P. M. (2014). Indian Ocean decadal variability: A review. *Bulletin of the American Meteorological Society*, *95*, 1679–1703.

Han, W., et al. (2010). Patterns of Indian Ocean sea-level change in a warming climate. *Nature Geoscience*, *3*, 546–550.

Hermes, J. C., et al. (2019). A sustained ocean observing system in the Indian Ocean for climate related scientific knowledge and societal needs. *Frontiers in Marine Science*, *6*, 355.

Hoerling, M., Hurrell, J. W., Xu, T., Bates, G., & Phillips, A. (2004). Twentieth century North Atlantic climate change. Part II: Understanding the effect of Indian Ocean warming. *Climate Dynamics*, *23*, 391–405.

Hood, R. R., Coles, V. J., Huggett, J. A., Landry, M. R., Levy, M., Moffett, J. W., & Rixen, T. (2024a). Chapter 13: Nutrient, phytoplankton, and zooplankton variability in the Indian Ocean. In C. C. Ummenhofer, & R. R. Hood (Eds.), *The Indian Ocean and its role in the global climate system* (pp. 293–327). Amsterdam: Elsevier. https://doi.org/10.1016/B978-0-12-822698-8.00020-2.

Hood, R. R., Rixen, T., Levy, M., Hansell, D. A., Coles, V. J., & Lachkar, Z. (2024b). Chapter 12: Oxygen, carbon, and pH variability in the Indian Ocean. In C. C. Ummenhofer, & R. R. Hood (Eds.), *The Indian Ocean and its role in the global climate system* (pp. 265–291). Amsterdam: Elsevier. https://doi.org/10.1016/B978-0-12-822698-8.00017-2.

Hu, S., & Fedorov, A. (2020). Indian Ocean warming as a driver of the North Atlantic warming hole. *Nature Communications*, *11*, 4785.

Kataoka, T., Tozuka, T., Behera, S., & Yamagata, T. (2014). On the Ningaloo Niño/Niña. *Climate Dynamics*, *43*, 1463–1482.
Kataoka, T., Tozuka, T., & Yamagata, T. (2017). Generation and decay mechanisms of Ningaloo Niño/Niña. *Journal of Geophysical Research, Oceans*, *122*, 8913–8932.
Kent, C., Chadwick, R., & Rowell, D. P. (2015). Understanding uncertainties in future projections of seasonal tropical precipitation. *Journal of Climate*, *28*, 4390–4413.
Kirtman, B., et al. (2013). Near-term climate change: Projections and predictability. In *Climate change 2013 the Physical Science Basis: Working group I contribution to the fifth assessment report of the Inter- Governmental Panel on Climate Change*.
Klein, S. A., Soden, B. J., & Lau, N. C. (1999). Remote sea surface temperature variations during ENSO: Evidence for a tropical atmospheric bridge. *Journal of Climate*, *12*, 917–932.
Knutson, T. R., et al. (2006). Assessment of twentieth-century regional surface temperature trends using the GFDL CM2 coupled models. *Journal of Climate*, *19*, 1624–1651.
Kosaka, Y., & Xie, S.-P. (2013). Recent global-warming hiatus tied to equatorial Pacific surface cooling. *Nature*, *501*, 403–407.
Kosaka, Y., & Xie, S. P. (2016). The tropical Pacific as a key pacemaker of the variable rates of global warming. *Nature Geoscience*, *9*, 669–673.
Kumar, P., Hamlington, B., Cheon, S.-H., Han, W., & Thompson, P. (2020). 20th century multivariate Indian Ocean regional sea level reconstruction. *Journal of Geophysical Research, Oceans*, *125*. e2020JC016270.
Lee, S., L'Heureux, M., Wittenberg, A. T., Seager, R., O'Gorman, P. A., & Johnson, N. C. (2022). On the future zonal contrasts of equatorial Pacific climate: Perspectives from observations, simulations, and theories. *npj Climate and Atmospheric Science*, *5*, 82.
Lee, S. K., Park, W., Baringer, M., Gordon, A. L., Huber, B., & Liu, Y. (2015). Pacific origin of the abrupt increase in Indian Ocean heat content during the warming hiatus. *Nature Geoscience*, *8*, 445–449.
Li, Y., & Han, W. (2015). Decadal Sea level variations in the Indian Ocean investigated with HYCOM: Roles of climate modes, ocean internal variability, and stochastic wind forcing. *Journal of Climate*, *28*, 9143–9165.
Li, Y., Han, W., & Zhang, L. (2017). Enhanced decadal warming of the Southeast Indian Ocean during the recent global surface warming slowdown. *Geophysical Research Letters*, *44*, 9876–9884.
Li, Y., Han, W., Zhang, L., & Wang, F. (2019). Decadal SST variability in the Southeast Indian Ocean and its impact on regional climate. *Journal of Climate*, *32*, 6299–6318.
Li, T., Wang, B., Chang, C. P., & Zhang, Y. (2003). A theory for the Indian Ocean dipole–zonal mode. *Journal of the Atmospheric Sciences*, *60*, 2119–2135.
Little, C. (2023). Coastal Sea level observations record the twentieth-century enhancement of decadal climate variability. *Journal of Climate*, *36*, 243–260.
Liu, Z. (2012). Dynamics of interdecadal climate variability: A historical perspective. *Journal of Climate*, *25*, 1963–1995.
Llovel, W., & Lee, T. (2015). Importance and origin of halosteric contribution to sea level change in the southeast Indian Ocean during 2005–2013. *Geophysical Research Letters*, *42*, 1148–1157.
Luo, J.-J., Sasakia, W., & Masumoto, Y. (2012). Indian Ocean warming modulates Pacific climate change. *Proceedings of the National Academy of Sciences of the United States of America*, *109*, 18701–18706.
McPhaden, M. J., Beal, L. M., Bhaskar, T.V.S. U., Lee, T., Nagura, M., Strutton, P. G., & Yu, L. (2024). Chapter 17: The Indian Ocean Observing System (IndOOS). In C. C. Ummenhofer, & R. R. Hood (Eds.), *The Indian Ocean and its role in the global climate system* (pp. 393–419). Amsterdam: Elsevier. https://doi.org/10.1016/B978-0-12-822698-8.00002-0.
Meehl, G. A., Covey, C., Delworth, T., Latif, M., McAvaney, B., Mitchell, J. F. B., Stouffer, R. J., & Taylor, K. E. (2007). The WCRP CMIP3 multi-model dataset: A new era in climate change research. *Bulletin of the American Meteorological Society*, *88*, 1383–1394.
Mohtadi, M., Abram, N. J., Clemens, S. C., Pfeiffer, M., Russell, J. M., Steinke, S., & Zinke, J. (2024). Chapter 19: Paleoclimate evidence of Indian Ocean variability across a range of timescales. In C. C. Ummenhofer, & R. R. Hood (Eds.), *The Indian Ocean and its role in the global climate system* (pp. 445–467). Amsterdam: Elsevier. https://doi.org/10.1016/B978-0-12-822698-8.00007-X.
Morioka, Y., Doi, T., & Behera, S. K. (2018). Decadal climate predictability in the southern Indian Ocean captured by SINTEX-F using a simple SST-nudging scheme. *Scientific Reports*, *8*, 1029.
Morioka, Y., Tozuka, T., & Yamagata, T. (2010). Climate variability in the southern Indian Ocean as revealed by self-organizing maps. *Climate Dynamics*, *35*, 1059–1072.
Newman, M., et al. (2016). The Pacific decadal oscillation, revisited. *Journal of Climate*, *29*, 4399–4427.
Nidheesh, A. G., Lengaigne, M., Vialard, J., Izumo, T., Unnikrishnan, A. S., & Krishnan, R. (2019). Natural decadal sea-level variability in the Indian Ocean: Lessons from CMIP models. *Climate Dynamics*, *53*, 5653–5673.
Nidheesh, A. G., Lengaigne, M., Vialard, J., Izumo, T., Unnikrishnan, A. S., Meyssignac, B., Hamlington, B., & de Boyer Montegut, C. (2017). Robustness of observation-based decadal sea level variability in the Indo-Pacific Ocean. *Geophysical Research Letters*, *44*, 7391–7400.
Nidheesh, A. G., Lengaigne, M., Vialard, J., Unnikrishnan, A. S., & Dayan, H. (2013). Decadal and long-term sea level variability in the tropical Indo-Pacific Ocean. *Climate Dynamics*, *41*, 381–402.
Nieves, V., Willis, J. K., & Patzert, W. C. (2015). Recent hiatus caused by decadal shift in Indo-Pacific heating. *Science*, *349*, 532–535.
Parker, D. E., Basnett, T. A., Brown, S. J., Gordon, M., Horton, E. B., & Rayner, N. A. (2000). Climate observations—The instrumental record. *Space Science Reviews*, *94*, 309–320.
Pierce, D. W., Barnett, T. P., AchutaRao, K. M., Glecker, P. J., Gregory, J. M., & Washington, W. M. (2006). Anthropogenic warming of the oceans: Observations and model results. *Journal of Climate*, *19*, 1873–1900.
Power, S., et al. (2021). Decadal climate variability in the tropical Pacific: Characteristics, causes, predictability and prospects. *Science*, *374*, eaay9165.
Rayner, N. A., Parker, D. E., Horton, E. B., Folland, C. K., Alexander, L. V., Rowell, D. P., Kent, E. C., & Kaplan, A. (2003). Global analyses of sea surface temperature, sea ice, and night marine air temperature since the late nineteenth century. *Journal of Geophysical Research*, *108*, 4407.

Reason, C. J. C. (2001). Subtropical Indian Ocean SST dipole events and southern African rainfall. *Geophysical Research Letters*, *28*, 2225–2227.

Reynolds, R. W., & Smith, T. M. (1994). Improved global sea surface temperature analyses using optimum interpolation. *Journal of Climate*, *7*, 929–948.

Roxy, M. K., Saranya, J. S., Modi, A., Anusree, A., Cai, W., Resplandy, L., … Frölicher, T. L. (2024). Chapter 20: Future projections for the tropical Indian Ocean. In C. C. Ummenhofer, & R. R. Hood (Eds.), *The Indian Ocean and its role in the global climate system* (pp. 469–482). Amsterdam: Elsevier. https://doi.org/10.1016/B978-0-12-822698-8.00004-4.

Roxy, M. K., Gnanaseelan, C., Parekh, A., Chowdary, J. S., Singh, S., Modi, A., Kakatkar, R., Mohapatra, S., Dhara, C., Shenoi, S. C., & Rajeevan, M. (2020). Indian Ocean warming. In R. Krishnan, J. Sanjay, C. Gnanaseelan, M. Mujumdar, A. Kulkarni, & S. Chakraborty (Eds.), *Assessment of climate change over the Indian region*. Singapore: Springer.

Roxy, M. K., Ritika, K., Terray, P., & Masson, S. (2014). The curious case of Indian Ocean warming. *Journal of Climate*, *27*, 8501–8509.

Saji, N. H., Goswami, B. N., Vinayachandran, P. N., & Yamagata, T. (1999). A dipole mode in the tropical Indian Ocean. *Nature*, *401*, 360–363.

Schwarzkopf, F., & Böning, C. (2011). Contribution of Pacific wind stress to multi-decadal variations in upper-ocean heat content and sea level in the tropical South Indian Ocean. *Geophysical Research Letters*, *38*, L12602.

Smith, D. M., Cusack, S., Colman, A. W., Folland, C. K., Harris, G. R., & Murphy, J. M. (2007). Improved surface temperature prediction for the coming decade from a global climate model. *Science*, *317*, 796–799.

Smith, D. M., et al. (2019). Robust skill of decadal climate predictions. *npj Climate and Atmospheric Science*, *2*, 13.

Sprintall, J., Biastoch, A., Gruenburg, L. K., & Phillips, H. E. (2024). Chapter 9: Oceanic basin connections. In C. C. Ummenhofer, & R. R. Hood (Eds.), *The Indian Ocean and its role in the global climate system* (pp. 205–227). Amsterdam: Elsevier. https://doi.org/10.1016/B978-0-12-822698-8.00003-2.

Srinivasu, U., Ravichandran, M., Han, W., Sivareddy, S., Rahman, H., Li, Y., & Nayak, S. (2017). Causes for the reversal of North Indian Ocean decadal sea level trend in recent two decades. *Climate Dynamics*, *49*, 3887–3904.

Sutton, R., McCarthy, G. D., Robson, J., Sinha, B., Archibald, A., & Gray, L. (2018). Atlantic multidecadal variability and the UK ACSIS program. *Bulletin of the American Meteorological Society*, *99*, 415–425.

Tanuma, N., & Tozuka, T. (2020). Influences of the interdecadal Pacific oscillation on the locally amplified Ningaloo Nino. *Geophysical Research Letters*, *47*. e2020GL088712.

Taylor, K. E., Stouffer, R. J., & Meehl, G. A. (2012). An overview of CMIP5 and the experiment design. *Bulletin of the American Meteorological Society*, *93*, 485–498.

Thompson, P. R., Piechch, C. G., Merrifield, M. A., McCreary, J. P., & Firing, E. (2016). Forcing of recent decadal variability in the equatorial and North Indian Ocean. *Journal of Geophysical Research, Oceans*, *121*, 6762–6778.

Timmermann, A., McGregor, S., & Jin, F.-F. (2010). Wind effects on past and future regional sea level trends in the southern Indo-Pacific. *Journal of Climate*, *23*, 4429–4437.

Tozuka, T., Luo, J. J., Masson, S., & Yamagata, T. (2007). Decadal modulations of the Indian Ocean dipole in the SINTEX-F1 coupled GCM. *Journal of Climate*, *20*, 2881–2894.

Trenberth, K. E., Branstator, G. W., Karoly, D., Kumar, A., Lau, N. C., & Ropelewski, C. (1998). Progress during TOGA in understanding and modeling global teleconnections associated with tropical sea surface temperatures. *Journal of Geophysical Research*, *103*, 14291–14324.

Ummenhofer, C. C., Taschetto, A. S., Izumo, T., & Luo, J.-J. (2024). Chapter 7: Impacts of the Indian Ocean on regional and global climate. In C. C. Ummenhofer, & R. R. Hood (Eds.), *The Indian Ocean and its role in the global climate system* (pp. 145–168). Amsterdam: Elsevier. https://doi.org/10.1016/B978-0-12-822698-8.00018-4.

Unnikrishnan, A. S., & Shankar, D. (2007). Are sea-level-rise trends along the coasts of the North Indian Ocean consistent with global estimates? *Global and Planetary Change*, *57*, 301–307.

Vialard, J. (2015). Hiatus heat in the Indian Ocean. *Nature Geoscience*, *8*, 423–424.

Xie, S. P., Deser, C., Vecchi, G. A., Ma, J., Teng, H., & Wittenberg, A. T. (2010). Global warming pattern formation: Sea surface temperature and rainfall. *Journal of Climate*, *23*, 966–986.

Xie, S.-P., Lu, B., & Xiang, B. (2013). Similar spatial patterns of climate responses to aerosol and greenhouse gas changes. *Nature Geoscience*, *6*, 828–832.

Xu, J., Luo, J.-J., & Yuan, C. (2022). Tropical Indian Ocean warming contributes to Arctic warming. *Geophysical Research Letters*, *49*. e2022GL101339.

Yamagami, Y., & Tozuka, T. (2015). Interdecadal changes of the Indian Ocean subtropical dipole mode. *Climate Dynamics*, *44*, 3057–3066.

Yan, L., Du, Y., & Zhang, L. (2013). Southern Ocean SST variability and its relationship with ENSO on inter-decadal time scales. *Journal of Ocean University of China*, *12*, 287–294.

Zhang, L., Han, W., Karnauskas, K. B., Li, Y., & Tozuka, T. (2022). Eastward shift of interannual climate variability in the South Indian Ocean since 1950. *Journal of Climate*, *35*, 561–575.

Zhang, L., Han, W., & Li, Y. (2018a). Mechanisms for generation and development of the Ningaloo Niño. *Journal of Climate*, *31*, 9239–9259.

Zhang, L., Han, W., Li, Y., & Lovenduski, N. (2019). Variability of sea level and upper-ocean heat content in the Indian Ocean: Effects of subtropical Indian Ocean dipole and ENSO. *Journal of Climate*, *32*, 7227–7245.

Zhang, Y., Feng, M., Du, Y., Philips, H., Bindoff, N., & McPhaden, M. J. (2018b). Strengthened Indonesian throughflow drives decadal warming in the southern Indian Ocean. *Geophysical Research Letters*, *45*, 6167–6175.

Zhang, Y., Wallace, J. M., & Battisti, D. S. (1997). ENSO-like interdecadal variability. *Journal of Climate*, *10*, 1004–1020.

Zheng, X.-T., Xie, S.-P., Vecchi, G. A., Liu, Q., & Hafner, J. (2010). Indian Ocean dipole response to global warming: Analysis of ocean–atmospheric feedbacks in a coupled model. *Journal of Climate*, *23*, 1240–1253.

Zhuang, W., Feng, M., Du, Y., Schiller, A., & Wang, D. (2013). Low-frequency sea level variability in the southern Indian Ocean and its impacts on the oceanic meridional transports. *Journal of Geophysical Research, Oceans*, *118*, 1302–1315.